

ELECTRONIC STRUCTURE OF MATERIALS CENTRE

ON THE NEED FOR A PARTIAL REVISION IN THE ORBITAL ASSIGNMENTS OF CYCLOPROPANE (C_3H_6)

M.J. Brunger and E. Weigold

**ON THE NEED FOR A PARTIAL REVISION IN THE ORBITAL
ASSIGNMENTS OF CYCLOPROPANE (C₃H₆)**

M.J. Brunger and E. Weigold†

Institute for Atomic Studies, School of Physical Sciences, The Flinders University of South
Australia GPO Box 2100, Adelaide, S.A., 5001, Australia

ABSTRACT

We report the results of an electron momentum spectroscopy (EMS) investigation into the orbital assignment for the two bands in the 15-18 eV binding energy range of the photoelectron spectrum of the saturated, 3-member ring hydrocarbon, cyclopropane (C₃H₆). The present experimental momentum distributions for these states provide compelling evidence that the earlier hypothesis of Schweig and Thiel [Chem. Phys. Lett. 21, 541 (1973)] is correct. That is, the orbital assignments of these two bands are in fact opposite to the sequence of the respective *ab initio* eigenvalues.

PACS number: 34.80 Dp

† Permanent Address: Research School of Physical Sciences and Engineering
Australian National University
GPO Box 4, Canberra, ACT 0200

Below a binding energy of about 20 eV the photoelectron spectrum (PES) of cyclopropane exhibits four bands [1]. The first two, both of which exhibit the effects of Jahn-Teller splitting [2], are well understood and are respectively classified as being due to the $2e'$ and $1e''$ molecular orbitals [3]. On the other hand, the origin of the two band maxima observed in the 15-18 eV range (bands 3 and 4) of the available PES spectra has been the subject of some controversy in the literature [1]-[3].

From their PES data Basch *et al.* [1] found that the maxima of bands 3 and 4 were separated by 0.8 eV and that there was a gap of ≈ 2.8 eV to the next lower maximum in their measured PES. Following the results of their *ab initio* calculations, which reproduced the gap in the molecular orbital (MO) energies, they postulated that band 3 should be attributed to the internal σ -MO ($2a_1'$ state) and that band 4 should be attributed to the σ CH-bonding ($1a_2''$ state) MO. However, subsequent to this [1], Schweig and Thiel [3] noted that the photoionisation cross section I_1 of the internal σ -MO is always predicted to be lower than the photoionisation cross section I_2 of the σ CH-bonding MO in the He I case, but higher in the He II case. Indeed in going from He I to He II excitation they calculated [3] that the ratio $\frac{I_1}{I_2}$ rises from 0.26 to 1.51. Further they argued that this most significant increase would be caused by the growth of the two-centre contributions from the bonding electrons in the internal σ -MO's which are concentrated about the centre of the ring and thus yield high overlap in the He II case. The intensity shift they expected was indeed seen in their measured He I and He II with the relative intensity of band 4 increasing sharply when they passed over to He II excitation. Accordingly, they concluded that band 4 should be ascribed to the internal σ -MO and band 3 to the σ CH-bonding MO i.e. opposite to the sequence of *ab initio* MO energies as proposed by Basch [1].

More recently Keller *et al.* [2] reported the results of their angle-resolved photoelectron spectroscopy study of C_3H_6 . Here values for the angular distribution parameter were reported as a function of photon energy for the first four bands of C_3H_6 . Unfortunately, their results proved to be somewhat ambiguous with respect to clarifying the conflicting

MO assignments of Basch *et al.* [1] and Schweig and Thiel [3] for bands 3 and 4. For instance, on the one hand their [2] $\Delta\beta$ value for band 4 lies within the range Kimura *et al.* [4] had previously established for the σ CH orbital classification, a result consistent with the interpretation of Basch *et al.* [1]. On the other hand the $\Delta\beta$ value they measured for band 3 was inconsistent with that established previously [5] for a σ -MO classification. Similarly, the magnitude for the near threshold $\beta(h\nu)$ curve of band 3, was not consistent with what one would expect [2] for σ -MO's.

Hence, the orbital assignments for bands 3 and 4 observed in the PES measurements [1]-[3] remain topical and we would argue that to clarify matters there is a clear need for the EMS measurement we now report. This is particularly true in this case as the beauty of the EMS technique is that it enables one to unequivocally determine the shape or "symmetry" of the respective momentum distributions for bands 3 and 4 and then by comparing them with our calculated plane wave impulse approximation-self consistent field (PWIA-SCF) momentum distributions [6] we can thus specify which band originates from the $1a_2''$ orbital and which band originates from the $2a_1'$ orbital, thereby resolving the current controversy in the literature.

A detailed description of the experimental apparatus and multiparameter coincidence techniques used in the present EMS investigation of C_3H_6 can be found in the review of McCarthy and Weigold [6]. Briefly, however, the present symmetric non-coplanar ($e,2e$) experiment [6] was conducted at a base energy of $E_0 = 1500$ eV and the overall (coincident) energy resolution was 1.7 eV (FWHM). The angular resolution was 1.3° (FWHM). Binding energy spectra were collected in the binning mode [6] in the region $\epsilon_f = 8 - 40$ eV at a number of different out-of-plane azimuthal angles ϕ and from a numerical deconvolution of these spectra the experimental momentum profiles were derived [6]. The present SCF wavefunction was constructed from the double zeta quality molecular wavefunction of Snyder and Basch [7] and was employed within the PWIA framework to calculate the current theoretical momentum distributions. A full report of this first EMS investigation

into the complete valence electronic structure of cyclopropane, which will include experimental and PWIA-SCF momentum distributions of each of the six valence orbitals of C_3H_6 , experimental and theoretical [8]-[9] pole strengths for each orbital and a detailed comparison between experiment and theory, will be given later [10]. For now we concentrate on peaks 3 and 4 (equivalent to bands 3 and 4 in the PES spectra) of figure 1, which illustrate examples of typical binding energy spectra as measured in the present study. Shown in figure 2 therefore are the summed $1a_2'' + 2a_1'$ PWIA-SCF momentum distribution (—), the individual PWIA-SCF $1a_2''$ (- - -) and $2a_1'$ (- · -) momentum distributions and the current summed experimental distribution of peaks 3 and 4 (●). Note the good agreement between the PWIA-SCF $1a_2'' + 2a_1'$ momentum distribution and the summed experimental momentum distribution for peaks 3 and 4 which clearly indicates that we have not missed any $1a_2''$ or $2a_1'$ flux in the deconvolution of the respective binding energy spectra. Also note that even though, for the sake of clarity, we have not shown the complete individual experimental momentum distributions for peaks 3 and 4 we found that the momentum profile of peak 3, whose centroid binding energy was $\epsilon_f = 15.7 \pm 0.1$ eV, was in quite good agreement with the PWIA-SCF result for the $1a_2''$ momentum distribution (- - -), whilst the momentum profile of peak 4, whose centroid binding energy was $\epsilon_f = 16.6 \pm 0.1$ eV, was in quite good agreement with the PWIA-SCF result for the $2a_1'$ momentum distribution (- · -). This is clearly seen in figure 2 where we have plotted the present EMS results for peak 3 (×) and peak 4 (□) that arose from the analysis [6] of the binding energy spectra in figure 1.

Consequently, consistent with the result of Schweig and Thiel [3], we conclude that the centroid binding energy of the $1a_2''$ orbital is at $\epsilon_f = 15.7 \pm 0.1$ eV and the centroid binding energy of the $2a_1'$ orbital is at $\epsilon_f = 16.6 \pm 0.1$ eV, opposite to the sequence of the respective *ab initio* eigenvalues. Finally, we further conclude, again consistent with reference [3], that the identified shortcomings of the *ab initio* results may be due to a failure in Koopmans' theorem [11] which does not allow for the effect of electronic reorganisation

upon ionisation in the calculation.

ACKNOWLEDGEMENTS

This work was supported in part by the Australian Research Council (ARC). One of us (MJB) also acknowledges the ARC for additional financial support.

REFERENCES

- [1] H. Basch, M.B. Robin, N.A. Kuebler, C. Baker and D.W. Turner, *J. Chem. Phys.* **51** (1969) 52.
- [2] P.R. Keller, J.W. Taylor, T.A. Carlson, T.A. Whitley and F.A. Grimm, *Chem. Phys.* **99** (1985) 317.
- [3] A. Schweig and W. Thiel, *Chem. Phys. Lett.* **21** (1973) 541.
- [4] K. Kimura, S. Katsumata, Y. Achiba, T. Yamazaki and S. Iwata, "Handbook of He(I) photoelectron spectra of fundamental organic molecules" (Halstead Press, New York, 1981).
- [5] P.R. Keller, J.W. Taylor, F.A. Grimm and T.A. Carlson, *Chem. Phys.* **90** (1984) 147.
- [6] i.E. McCarthy and E. Weigold, *Rep. Prog. Phys.* **54** (1991) 789.
- [7] L.C. Snyder and H. Basch, "Molecular Wavefunctions and Properties" (Wiley, New York, 1972).
- [8] L.S. Cederbaum, W. Domcke, J. Schirmer, W. von Niessen, G.H.F. Diercksen and W.P. Kraemar, *J. Chem. Phys.* **69** (1978) 1591.
- [9] W. von Niessen and V.G. Zakrzewski, private communication (1993).
- [10] M.J. Brunger and E. Weigold, *Chem. Phys.* (1994) to be submitted.
- [11] T. Koopmans, *Physica* **1** (1934) 104.

FIGURE CAPTIONS

Figure 1: The 1500 eV non-coplanar symmetric EMS binding energy spectra of C_3H_6 at $\phi = 0^\circ$ and $\phi = 9^\circ$. The curves show the fitted spectra using the known energy resolution function.

Figure 2: The present 1500 eV non-coplanar symmetric PWIA-SCF momentum distribution for the $1a_2'' + 2a_1'$ states (—) compared against our corresponding experimental data (\bullet). Also shown are the respective $1a_2''$ (- - -) and $2a_1'$ (· · · ·) PWIA-SCF state contributions and the present EMS results, from the binding energy spectra of figure 1, for peak 3 (\times) and peak 4 (\square), respectively.

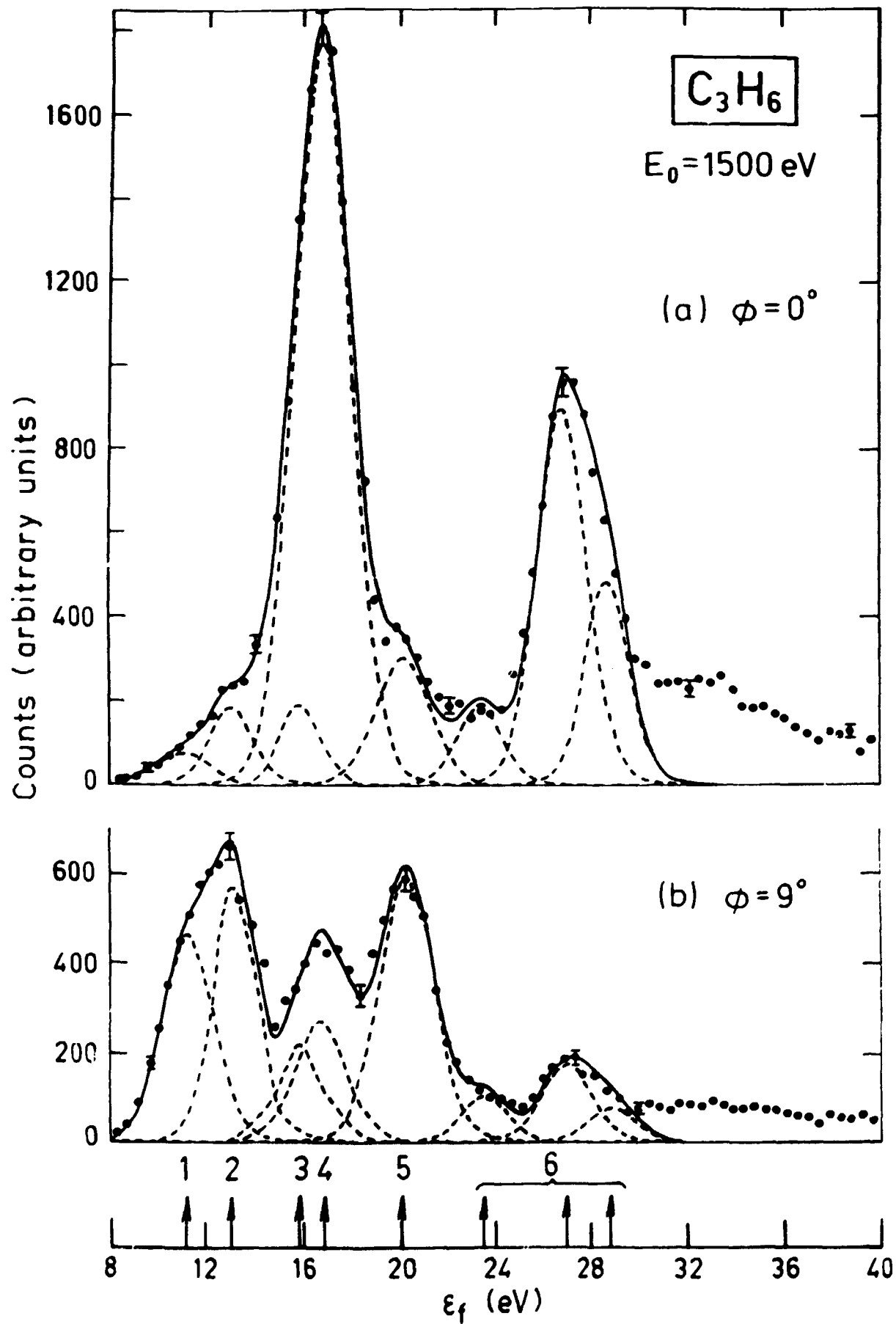


Figure 1

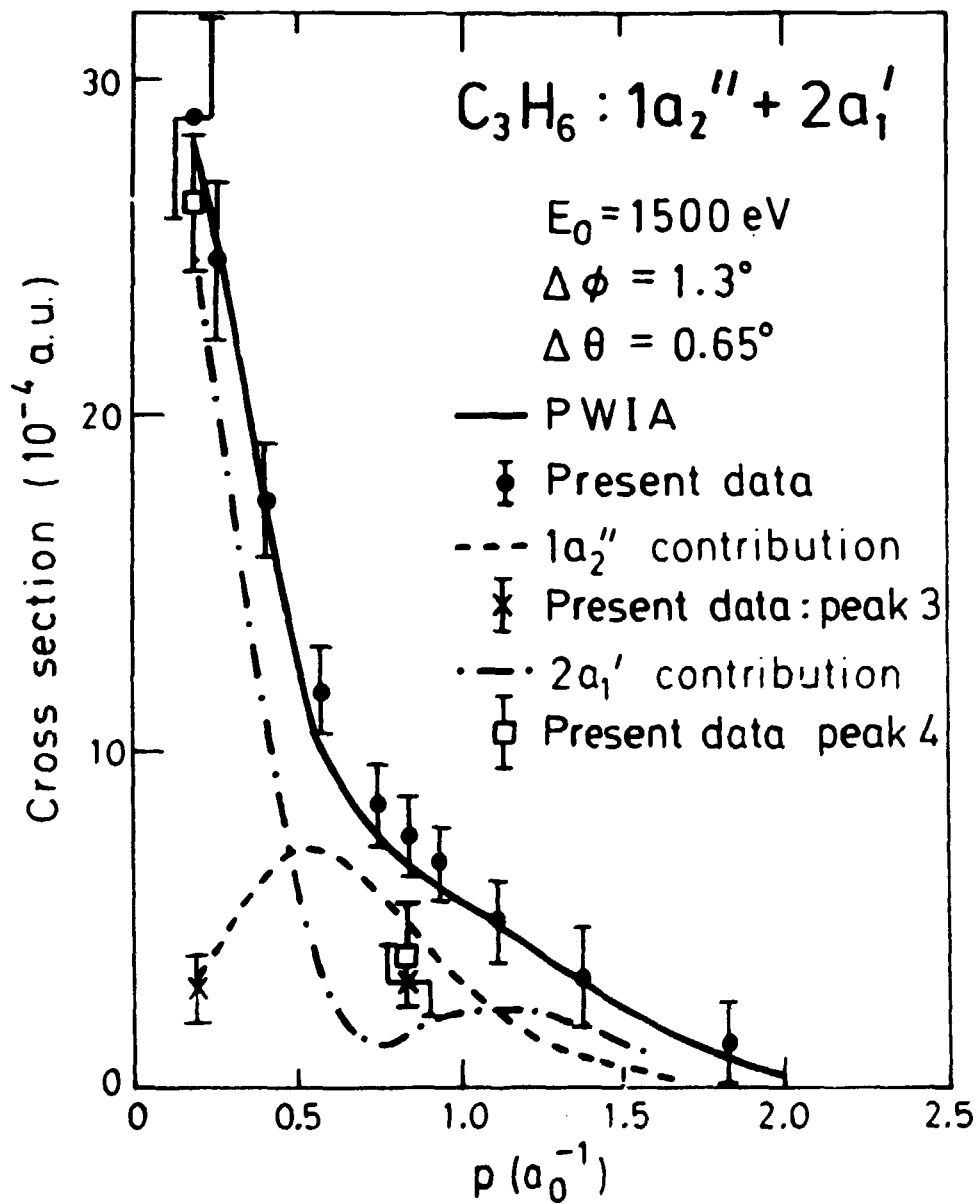


Figure 2